Morphological and functional development of the spiral intestine in cloudy catshark (*Scyliorhinus torazame*)

Yuki Honda[1,*], Wataru Takagi[1], Marty K. S. Wong[1], Nobuhiro Ogawa[1], Kotaro Tokunaga[2], Kazuya Kofuji[2], and Susumu Hyodo[1]

[1]Atmosphere and Ocean Research Institute, The University of Tokyo, Kashiwa, Chiba 277-8564, Japan

[2]Ibaraki Prefectural Oarai Aquarium, Oarai, Ibaraki 311-1301, Japan

*Author for correspondence (honda@aori.u-tokyo.ac.jp)

Keywords: Spiral intestine, Pre-hatching, Embryonic nutrition, PepT1, Slc6a19, Oviparous cartilaginous fish

ABSTRACT

Cartilaginous fish have a comparatively short intestine known as the spiral intestine that is comprised of a helical spiral of intestinal mucosa. However, morphological and functional development of the spiral intestine is not well described. Unlike teleosts, cartilaginous fish are characterized by an extremely long developmental period *in ovo* or *in utero* for example; in the oviparous cloudy catshark (*Schyliorhinus torazame*), the developing fish remains inside the egg capsule for up to six months, suggesting that the embryonic intestine may become functional prior to hatch. In the present study, we describe the morphological and functional development of the spiral intestine in the developing catshark embryo. Spiral formation of embryonic intestine was completed at the middle of stage 31, prior to "pre-hatching", which is a developmental event characterized by the opening of egg case occurring at the end of the first third of development. Within 48 hours after pre-hatching event, egg yolk began to flow from the external yolk sac into the embryonic intestine via the yolk stalk. At the same time, there was a rapid increase in mRNA expression of the peptide transporter *pept1* and neutral amino acid transporter *slc6a19*. Secondary folds in the intestinal mucosa and microvilli on the apical membrane appeared after pre-hatching, further supporting the onset of nutrient absorption in the developing intestine at this time. We demonstrate the acquisition of intestinal nutrient absorption at the pre-hatching stage of an oviparous elasmobranch.

INTRODUCTION

Cartilaginous fish (sharks, rays and chimaeras) have evolved many unusual physiological features, including aspects of osmoregulation (Smith, 1936; Hyodo et al., 2014), reproduction (Musick and Ellis, 2005) and gastrointestinal morphology (Wilson and Castro, 2010). The spiral intestine is considered to be a plesiomorphic feature of vertebrate and is found in the non-teleostean actinopterygii, non-tetrapod sarcopterygii, elasmobranchii and holocephalii (Argyriou et al., 2016). The comparatively short intestine in these fishes is offset by the spiral arrangement of the mucosa (Khanna, 2004), significantly increasing the surface area of the intestine up to three and six-fold depending on morphology and species (Bertin 1958). One explanation for the physiological advantage of the spiral intestine in elasmobranchs is to maximize intestinal surface area in a limited body space that is dominated by a large lipid dense liver (White, 1937). Digesta rotate along the longitudinal axis of the intestine, resulting in a slower evacuation time and further increasing absorptive capacity (Wetherbee et al., 1987). In cartilaginous fishes, the anatomy of the intestine has been well described in several species of shark and ray (Perrault, 1671; Parker, 1880; Khanna, 2004; Chatchavalvanich et al., 2006), and the spiral structures have been classified as spiral, ring or scroll type (White, 1937; Compagno et al., 2005; Leigh et al., 2017). However, we know little regarding the morphological and functional development of the intestine in elasmobranchs.

Unlike teleosts, cartilaginous fish are characterized by an extremely long developmental period *in ovo* or *in utero*. During early development, the richly vascularized yolk-sac membrane contributes to absorption of nutrients by the developing embryos (Jollie and Jollie, 1967, Hamlett et al., 2011; Conrath and Musick, 2012). In viviparous species, embryos begin to use the gastrointestinal tract around the middle of

gestation. In southern stingray (*Dasyatis americana*), lipid rich histotroph known as uterine milk is secreted by the uterine villi and embryos drink the milk *in utero* (Hamlett et al., 1996), and in the crocodile shark (*Pseudocarcharias kamoharai*), embryos ingest trophic eggs *in utero* (Fujita, 1981). Conversely, oviparous embryos depend entirely on yolk, however, this has been shown to be present within the lumen of the embryonic intestine during development (Lechenault et al., 1993; Haines et al., 2005). In the oviparous lesser spotted dogfish (*Scyliorhinus canicula*), yolk internalization occurred approximately after the first third of embryonic life (Ballard et al. 1993) and in the ovoviviparous spiny dogfish (*Squalus acanthias*) yolk was firstly observed in the intestinal lumen of 70 mm length embryo, and then fat droplets were observed in intestinal epithelial cells when the embryos were approximately 150 mm in length (Tewinkel, 1943). These findings raise the hypothesis that, even in oviparous elasmobranchs, the spiral intestine is formed and most likely functional for nutrient absorption well before hatch (Tewinkel, 1943; Rodda and Seymour, 2008). In the present study, we focused on the timing of the "pre-hatching" event in the onset of nutrient absorption by the embryonic intestine. Pre-hatching occurs in oviparous elasmobranchs at the end of the first third of development and is a period when the egg casing is known to open to the environment to facilitate embryonic respiration and growth (Mellinger et al., 1986; Diez and Davenport, 1987; Mellinger et al., 1989). This hypothesized developmental trajectory is distinctly different from oviparous ray-finned fishes that typically hatch before complete development of the gastrointestinal tract (Ng et al., 2005). Unraveling the functional development of the spiral intestine is thus important for our understanding of embryonic growth in cartilaginous fish.

In the present study, we describe the functional development of the spiral

intestine in the oviparous cloudy catshark (*Scyliorhinus torazame*). To this end, we investigated; 1) formation of the spiral structure, esophageal opening and rectum opening, 2) formation of the secondary folds and microvilli that are related to nutrient absorption, and 3) the timing of when yolk first appears in the embryonic intestine. In addition, as protein is a major diet component in fishes (Clements and Raubenheimer, 2006) and peptide transporter 1 (PepT1) and the neutral amino acid transporter (Slc6a19) are known to contribute to nutrient absorption across the teleost intestine (Verri et al., 2003; Rønnestad et al., 2007; Terova et al., 2009; Rimoldi et al., 2015; Xu et al., 2016; Orozco et al., 2017; Orozco et al., 2018), we also examined spatiotemporal expression of mRNAs encoding PepT1 and Slc6a19 in the intestine as functional gene expression markers. We provide evidence of a functional intestine in the oviparous cloudy catshark shortly after the pre-hatching event, suggesting that pre-hatching represents a physiological turning point in the embryonic development of oviparous cartilaginous fish.

MATERIALS AND METHODS

Animals

Spawned cloudy catshark (*S. torazame*) eggs collected from captive individuals were transported from Ibaraki Prefectural Oarai Aquarium to the Atmosphere and Ocean Research Institute, The University of Tokyo. They were kept in a 1000 L tank with recirculating natural seawater under a constant photoperiod (12 h:12 h, light:dark) at 16°C.

Embryos were staged according to the developmental stages established in lesser spotted dogfish, *S. canicula* (Ballard et al., 1993). Approximately 2 months post fertilization at the end of the first third of development classified as the middle of developmental stage 31, the anterior part of the egg capsule opens and is known as the "pre-hatching" or "eclosion" (Ballard et al., 1993; Takagi et al., 2017). For our experiment, we further subdivided this stage into two phases: the first half prior to pre-hatch (stage 31 Early or 31E) and the second half post pre-hatch (stage 31 Late or 31L). Occurrence of pre-hatching was confirmed by gentle pressure on the egg capsule, if intracapsular fluid was released pre-hatching had occurred. Once hatched juveniles were maintained under similar environmental conditions and fed a diet of chopped squid twice a week *ad libitum*. Embryos and juveniles were sampled throughout the year in 2015 to 2020. For sampling, both embryos and juveniles were anesthetized in 0.02% ethyl 3-aminobenzoate methanesulfonate (Sigma-Aldrich, St. Louis, MO, USA). All animal experiments were conducted according to the Guidelines for Care and Use of Animals approved by the committee of The University of Tokyo (A16-13).

Histological observation

The embryos from developmental stage 23 to 34 and juveniles were used for histological observation. For juveniles and embryos at developmental stages 32, 33 and 34, spiral intestines were dissected out, and were fixed in formalin with picric acid (saturated picric acid:formalin = 3:1) at 4°C overnight. Spiral intestines of embryos earlier than stage 32 were fixed *in toto*. Fixed tissues were washed twice in 70% ethanol, dehydrated in graded concentrations of ethanol, cleared with benzene, and embedded in Paraplast (McCormick Scientific, Richmond, IL, USA). Serial sections were cut at 6 µm thickness and mounted onto glass slides (Matsunami Glass, Osaka, Japan). The sections were stained with hematoxylin and eosin. First, rehydrated tissue sections were treated with hematoxylin solution (Wako Pure Chemical Industries, Osaka, Japan) for 5 min and then washed in running tap water for 30 min. The sections were then stained with eosin (Chroma Gesellschaft Schmidt, Koengen, Germany) for 10 min, dehydrated through graded concentrations of ethanol, cleared with xylene, and were mounted with Permount (Thermo Fisher Scientific, Waltham, MA, USA). Micrographs were obtained using a digital camera (DSRi1; Nikon, Tokyo, Japan). For 3D reconstruction of the developing spiral intestine, sequential images of serial sections of the intestine were aligned using ImageJ software ver. 1.52i (Schindelin et al., 2012) and the luminal space of intestine was filled using Photoshop (Adobe Systems, San Jose, CA, USA) before a 3D image was created using the 3D viewer of the ImageJ.

Scanning electron microscopy

For scanning electron microscopy observation, embryos of stages 27, 31E and 32, and juveniles were examined. After dissection, spiral intestines of juveniles and embryos of stages 31E and 32 were pre-fixed in a fixative containing 2% paraformaldehyde and 2.5% glutaraldehyde in 0.05 M Cacodylate Buffer (CB, pH 7.4) (PG solution) for 3 min to harden the surface of tissue. Tissue samples were cut using a razor blade and then fixed again in the PG solution for 2 h. After washing in 0.05 M CB for 5 min, samples were fixed in 1% osmium tetroxide for 1 h, washed in 0.05 M CB, dehydrated through a graded concentration of ethanol, immersed in butyl alcohol, and then dried in a vacuum freeze-dryer (JFD-300, JEOL Ltd., Tokyo, Japan) overnight. Tissues mounted on a sample holder were coated with platinum palladium using ion sputtering apparatus (E-1030, Hitachi High-Technologies Corporation, Tokyo, Japan) and were kept in a vacuum desiccator until use.

Due to the small size of samples, the intestine from stage 27 embryos were cryosectioned to expose the gut cavity. The embryos were pre-fixed in the PG solution for 30 min. After washing in 0.05 M CB, samples were immersed at 4°C in 10% glucose in 0.05M CB for 10 min, 20% glucose for 30 min, 30% glucose for 40 min, OCT compound (Sakura Finetek Japan, Tokyo, Japan) for 30 min, and were then frozen in new OCT compound. Blocks were sliced at 5 µm using a cryostat until the intestinal lumen was exposed. After rinsing the residual OCT compound in 0.05 M CB and post-fixation in the PG solution for 2h, tissues were processed for scanning electron microscopy as mentioned above. All observations were made using a scanning electron microscope (s-4800, Hitachi High-Technologies Corporation) at a magnification of 10,000x or 20,000x.

cDNA cloning

Complementary DNA cloning was performed as previously described in detail (Takagi et al., 2017) using whole spiral intestine dissected from juvenile cloudy catsharks. Total RNA was extracted using a commercially available kit (ISOGEN, Nippon Gene, Toyama, Japan). One µg DNase-treated total RNA was reverse-transcribed to first-strand cDNA using an iScript cDNA Synthesis Kit (Bio-Rad, Hercules, CA, USA), following the manufacturer's instructions. Putative nucleotide sequences of mRNAs encoding catshark PepT1, Slc6a19 and β-actin were obtained by BLAST search on catshark transcriptome database, Squalomix (https://transcriptome.riken.jp/squalomix/) (Hara et al., 2018). Partial cDNA fragments, which were amplified with Kapa Taq Extra DNA polymerase (Kapa Biosystems, Boston, MA, USA) and gene specific primer sets (Table S1), were ligated into pGEM-T Easy plasmid vector (Promega, Madison, WI, USA). The nucleotide sequences were determined by a DNA sequencer (ABI PRISM 3130, Life Technologies, Carlsbad, CA, USA).

Molecular phylogenetic analysis

Molecular phylogenetic analyses were conducted in MEGA7 (Kumar et al., 2016). The deduced amino acid sequences of catshark PepT1 and Slc6a19 were aligned with those of other animals using MUSCLE (Edgar, 2004). Molecular phylogenetic trees were inferred by using the Maximum Likelihood method based on the Le_Gascuel_2008 model. A discrete Gamma distribution was used to model evolutionary rate differences among sites (5 categories (+G, parameter = 0.4843)). The bootstrap number was set to 1000.

Real-time quantitative PCR assay

Whole intestine was obtained from juveniles and embryos of stages 31E, 31L, 32, 33 and 34. Intestines were divided equally along the longitudinal axis into three parts, anterior, middle, and posterior. Total RNA extraction and first-strand cDNA synthesis were conducted as described above. Quantitative PCR (qPCR) was performed using a 7900 HT Sequence Detection System (Life Technologies) with KAPA SYBR Fast qPCR Kit (Kapa Biosystems), as previously described in detail (Hasegawa et al., 2016). The primers used for real-time qPCR were designed using PrimerQuest (http://sg.idtdna.com/primerquest/home/index) (Table S1). β-actin mRNA was used as an internal control (Takagi et al., 2017). The plasmids containing cloned cDNA fragments were used as the known amounts of standard templates for absolute quantification in qPCR analyses.

***In situ* hybridization**

Digoxigenin (DIG)-labeled cRNA probes were synthesized from plasmids containing PepT1 and Slc6a19 coding sequences with DIG RNA Labeling Kit (Roche Applied Science, Mannheim, Germany). Tissue sections were mounted onto MAS-GP-coated glass slides (Matsunami). Hybridization was conducted using a previously described protocol (Takabe et al., 2012). In brief, deparaffinized sections were treated with 5 µg/mL Proteinase K (Sigma) in PBS for 10 min at 37°C, immersed in prehybridization buffer [5x SSC (0.75 M NaCl and 83.3 mM sodium citrate, pH 7.0), 50% formamide] at 58°C, hybridized with DIG-labeled cRNA probes in hybridization buffer (50% formamide, 5x SSC, 40 µg/mL bovine calf thymus DNA) at 58°C for 40 h.

Sections were then washed in 2x SSC for 30 min at room temperature, 2x SSC for 1 h at 65°C, and in 0.1x SSC for 1 h at 65°C. After incubation with alkaline phosphatase-conjugated anti-DIG antibody (Roche) for 2 h at room temperature, signals were visualized with 4-nitro blue tetrazolium chloride (450 mg/ml) and X-phosphate/ 5-bromo-4-chloro-3-indolyl-phosphate (175 mg/ml) until sections were colored at 25°C in the dark condition. Sections were counterstained with Nuclear Fast Red (Vector Laboratories Inc., Burlingame, CA, USA).

Statistical analysis

Data are expressed as mean ± s.e.m. Statistical analyses were conducted using Kyplot5.0 software (KyensLab Inc., Tokyo, Japan). Normality of data was checked by Shapiro-Wilk test, followed by a Steel-Dwass or Tukey-Kramer's multiple comparison test. *P*-values less than 0.05 were considered statistically significant.

RESULTS

Formation of spiral structure during development

Catshark embryos continued to develop inside the egg capsule for approximately 6 months prior to hatch (Figs. 1A-E). Histological investigation revealed that the spiral structure of intestine was fully formed prior to the pre-hatching period. At stage 23 of embryonic development (approximately 1 month post fertilization), a straight intestinal tract was visible in the body cavity, which consisted of pseudostratified epithelium and mesenchyme (Fig. 1F). At stage 24, two-separated intestinal lumens were observed in sagittal sections, showing the presence of one or two spiral turns (Fig. 1G, O). The number of turns continued to increase after stage 24 (Figs. 1H-J). At stage 31E, the number of spiral turns reached seven (Fig. 1K) which is equal to that of juveniles (Fig. 1L). The number of spiral turns was confirmed by 3D reconstruction using serial sections (Figs. 1M, N).

Yolk inflow into the intestine

At stage 23 in development, the yolk inside the external yolk sac (EYS) was black, and the embryo and the yolk stalk were transparent under transmitted light (Fig. 2A). At stage 24, sagittal sections revealed that the lumen of the yolk stalk was directly connected with the intestinal lumen (Fig. 2B, dotted line), however, a monolayer cellular membrane prevented yolk from flowing into the yolk stalk (Fig. 2C, arrows). At development stage 31E, yolk was not observed in the intestinal lumen (Fig. 2D), however, at stage 31L, white yolk was visible inside the yolk stalk (Fig. 2E, arrow) and eosinophilic yolk granules were observed in the intestine (Fig. 2F, arrow).

To determine the precise timing of yolk inflow into the embryonic intestine, we further examined four individuals, the developmental stages of which were within 48 hours after pre-hatching. Within 24 h after pre-hatching, one embryo had no yolk (Fig. S1A), while a second individual showed yolk granules inside the intestinal lumen (Fig. S1B). At 36-48 hours after pre-hatching, two embryos had yolk granules inside the intestinal lumen (Figs. S1C, D), implying that yolk inflow into the intestine likely occurs within 48 hours after pre-hatching.

Formation of secondary folds and microvilli

Intestinal epithelium remained smooth without folding until pre-hatching (Figs. 3A, C), but in some individuals, a slight protrusion of the intestinal epithelium was observed around the pre-hatching event, and obvious secondary folds were confirmed at stage 32 (Fig. 3E, arrows). The length of secondary folds gradually increased as the animal grew (Figs. 3E, G) and elongated secondary folds (Fig. 3G) and dense microvilli (Fig. 3H) were observed in the juvenile stage post-hatch. Microvillus formation began prior to secondary folds formation. Short microvilli were sparsely distributed in the stage 27 embryo (Fig. 3B, arrows). At stage 31E, microvilli covered the apical surface of the intestinal lumen (Fig. 3D) and both density and length of the microvilli increased in the juvenile stage (Figs. 3F, H).

Esophagus formation and opening

At stage 25, the esophagus was cylindrical in structure filled with mesenchyme and it could be distinguished from oral cavity and stomach (Figs. 4A, B). At stage 27, the luminal epithelium was differentiated, but the esophagus remained closed (Figs. 4C, D, arrowheads). By stage 33, the esophagus appeared closed by adhering the dorsal and ventral sides of epithelia (Figs. 4E, F), however, this adhesion seemed not to be tight as some gaps were sparsely observed (Fig. 4F, arrows). The leaky but closed esophagus was observed also in the stage 34 embryo (Fig. 4H, arrows), and the closed portion became narrower longitudinally at this stage (Fig, 4G). We confirmed the opening of esophagus in fed juvenile (Figs. 4I, J).

Connection between spiral intestine and rectum

In the lesser spotted dogfish embryo, the rectum was shown to be closed until hatch (Mellinger et al., 1986; 1987). The serial transverse sections from the end of the spiral intestine to the rectum revealed that the lumen of the rectal canal, which forms the junction between the spiral intestine (fig. 5C) and the rectum (Fig. 5E), was not fully developed and closed at stage 34 (Fig. 5D). In the hatched juvenile, formation of the rectal canal is completed, and the lumen was continuously formed from the spiral intestine to the rectum (Figs, 5H-J).

Spatiotemporal expression of *pept1* and *slc6a19* mRNAs

By searching the catshark transcriptome database, contigs showing high homology to *pept1* and *slc6a19* were found, and fragments of cDNAs encoding the catshark PepT1 and Slc6a19 were cloned. The accession numbers for the partial sequences of catshark *pept1* and *slc6a19* are LC507941 and LC507942, respectively. Maximum-likelihood analysis clearly show that the catshark cDNAs belong to the vertebrate *pept1* (*slc15a1*) and *slc6a19* lineages, respectively (Fig. 6).

To evaluate nutrient absorptive function of embryonic intestine, expression of *pept1* and *slc6a19* mRNAs were examined by quantitative RT-PCR (qPCR) and *in situ* hybridization (Figs. 7-9). Low levels of *pept1* mRNA expression were detected at stages 31E and 31L (Fig. 7A). The expression levels significantly increased at stage 32, and thereafter remained high until the juvenile stage. *slc6a19* mRNA showed relatively low levels of expression during the embryonic period, and showed an increasing trend in expression in juveniles, although the changes between stages were statistically insignificant (Fig. 7B).

In the Mozambique tilapia, expression of *pept1* mRNA was shown to be rich in the anterior region of the intestine (Orozco et al., 2017), therefore, we divided the spiral intestine into anterior, middle and posterior sections, and examined regional expression of *pept1* and *slc6a19* mRNA. *pept1* mRNA was uniformly distributed throughout the spiral intestine at and before stage 33, whereas, from stage 34 onward expression of *pept1* mRNA was higher in the anterior region of the spiral intestine compared to the posterior region (Fig. 8A). Consistent with the results of qPCR, moderate signals were found in the entire region of intestine at stage 32 by *in situ* hybridization, and anteriorly-biased signals

were shown as developmental stage progressed (Figs. 9A, E, I). In the juvenile intestine, *pept1* mRNA showed intense signals in secondary folds constituting the 1st and 2nd spiral turns (Fig. 9M) and moderate levels of *pept1* mRNA signals were observed in the epithelial cells of 3rd to 5th spiral turns, but signals were faint in the posterior part of spiral intestine. The *pept1* mRNA signals were limited to the epithelial cells (Figs.9B, F, J, N, arrowheads) and no expression was observed in submucosa.

Expression of *slc6a19* mRNA exhibited different patterns compared to *pept1* mRNA (Fig. 8B). At stage 32, mRNA levels of *slc6a19* in the anterior region were significantly higher compared to that in the middle region. At stage 33, expression of *slc6a19* increased in the posterior region gradually and became significantly higher at stage 34. In the juvenile intestine, no difference was observed in *slc6a19* mRNA levels among the three regions. In agreement with the results of qPCR, the posterior most region showed strong signals for *slc6a19* mRNA in the intestine of stage 34 embryos by *in situ* hybridization (Fig. 9K, arrow). Intense mRNA signals for *slc6a19* were shown in secondary folds throughout the juvenile intestine (Fig. 9O). The *slc6a19* mRNA signals were limited to the epithelial cells (Figs. 9D, H, L, P, arrowheads).

DISCUSSION

Here we have demonstrated that spiral formation of the intestine completed before pre-hatching in the cloudy catshark. We further revealed the presence of yolk in the intestine and expression of key nutrient transporters after pre-hatching. Our data suggest a switch from nutrient absorption via the yolk sac membrane to the intestine at the pre-hatching stage, which likely facilitates growth and development of the embryo inside the egg case.

Before the pre-hatching event: spiral intestine formation

The presence of a spiral intestine in developing embryos has been shown in several elasmobranch species including the round stingray *Urobatis helleri* (Babel, 1966), lesser spotted dogfish (Ballard et al., 1993) and tropical whitespotted bamboo shark *Chiloscyllium plagiosum* (Xu et al., 2015), but detailed spiral formation and functional relevance of the spiral intestine during embryonic development were unknown. Recently, detailed morphogenesis of the spiral intestine was reported in little skate *Leucoraja erinacea* using histology and microCT scan (Theodosiou and Oppong, 2019). In the little skate, spiral formation began at stage 25, and the number of spiral turns reached 6.5 by stage 30, the number of spiral turns in embryos at the final developmental stage (stage 34; more than 14 weeks after stage 30) was 8, equivalent to that in adult individual (Theodosiou and Oppong, 2019); however, the number of spiral turns at pre-hatching was not reported so we are unable to compare the exact timing of complete spiral formation between the cloudy catshark and little skate. Currently the present study is the only study showing that spiral formation of the intestine is completed before pre-hatching in an elasmobranch. Further studies in other species are needed to confirm whether our finding

on the spiral formation is common in all cartilaginous fish.

In addition to spiral formation, microvillus formation was observed prior to pre-hatching. Short microvilli were sparsely distributed from stage 27, and microvilli covered the apical surface of the intestinal lumen at stage 31E, but intestinal epithelium remained smooth without folding until pre-hatching. In vertebrate intestines, it is generally accepted that three morphogenetic processes occur continuously to maximize surface area for nutrient absorption: 1) elongation of the gut tube, 2) microvilli formation, and 3) villi or secondary fold formation (Walton et al., 2016). In the zebrafish embryo, microvilli formation starts at 74 hours post fertilization (hpf) (Wallace et al., 2005), whereas secondary fold formed around 96 hpf (Ng et al., 2005). Spiral formation in the cartilaginous fish intestine could be considered to be functionally equivalent to the elongation of gut tube in terms of an increase in luminal surface area. Therefore, it could be hypothesized that the described series of morphogenetic processes in the intestine may be common across jawed vertebrates.

After the pre-hatching event: nutritional absorption in the embryonic intestine

After the pre-hatching event, obvious secondary folds were found at stage 32, and the length of secondary folds, as well as the length and the density of microvilli, increased as the embryo grew. However, the most prominent change that occurred before and after the pre-hatching event was the presence of yolk in the embryonic intestine. Lechenault et al. (1993) reported that yolk transfer begins within one week of pre-hatching in the lesser spotted dogfish embryo. In our detailed observation, yolk transfer occurred within 48 hours after pre-hatching. This variation may be due to a difference in incubation temperature of eggs (14°C in the previous study, while 16°C in our study).

Yolk transfer from the EYS into the embryonic intestine is considered to be driven by cilia on the epithelium of EYS and the yolk stalk (Tewinkel, 1943), however, we identified a membrane preventing the movement of yolk into the intestine prior to pre-hatching. As the appearance of yolk occurs at pre-hatching, it can be assumed that the collapse of this membrane may be tightly regulated possibly by signals released from the maturing intestine.

Our morphological findings are consistent with the previous histological observation showing that intestinal epithelial cells of elasmobranch embryos have the ability to absorb nutrients (Tewinkel, 1943; Okano et al., 1981; Teshima and Tomonaga, 2016). To further confirm nutrient absorption from the embryonic intestine, we examined expression of mRNAs encoding a peptide transporter (PepT1) and a neutral amino acid transporter (Slc6a19) as functional markers for nutrient absorption (Clements and Raubenheimer, 2006). The cDNA encoding PepT1 was previously cloned from the intestine of the bonnethead shark, *Sphyrna tiburo* (Hart et al., 2016), and we show the anterior-biased expression of *pept1* mRNA at stage 34 and juvenile spiral intestines of the cloudy catshark. This bias in expression is consistent with the distribution of *pept1* mRNAs in teleosts, such as European sea bass *Dicentrarchus labrax* (Terova et al., 2009), turbot *Scophthalmus maximus* (Xu et al., 2016) and tilapia *Oreochromis mossambicus* (Orozco et al., 2017). Zebrafish *Danio rerio* and grass carp *Ctenopharyngodon idella* show proximally-restricted expression of *pept1* mRNA (Verri et al., 2003; Liu et al., 2013). These results imply that *pept1* mRNA in the intestine generally shows expression pattern in anterior-biased fashion in fish. However, ubiquitous *pept1* mRNA expression has been shown in Atlantic cod *Gadus morhua* and killifish *Fundulus heteroclitus macrolepidotus* (Bucking and Schulte, 2012; Rønnestad et al., 2007). In our observations, *pept1* mRNA

was initially expressed broadly throughout the entire intestine in early developmental stages, but the expression of *pept1* was restricted to the anterior intestine as development proceeded. A similar change in mRNA expression patterns (broader in larva) was also reported in the Japanese eel *Anguilla japonica* (Ahn et al., 2013). Expression pattern of *pept1* mRNA seems to be plastic depending on ontogeny, physiological condition or species.

Transporters contributing to amino acid absorption include a number of proteins that have distinct substrate specificities to neutral, basic and acidic amino acids (Bröer, 2008). In the present study, we selected a neutral amino acid transporter Slc6a19 as the indicator of amino acid absorption due to the importance of neutral amino acids for maintaining body homeostasis (Bröer et al., 2004; Sveier et al., 2001; Craig and Moon, 2013; Belghit et al., 2014). The Slc6a19 is a major neutral amino acid transporter expressed in the vertebrate intestine, and mutations in *slc6a19* gene cause an inherited autosomal recessive defect known as Hartnup disorder (Kleta et al., 2004). Expression of *slc6a19* mRNA was found throughout the juvenile intestine a pattern similar to that shown in the European sea bass and turbot (Rimoldi et al., 2015; Xu et al., 2016). Aminopeptidase activity was shown to peak in the mid spiral intestine of young adults or late juveniles of bonnethead sharks (Jhaveri et al., 2015), suggesting that peptides not absorbed in the anterior region may be digested by aminopeptidases and then absorbed in the form of free amino acids across the posterior region. In accordance with this notion, a remarkable expression of *slc6a19* mRNA was observed in the most posterior part of the intestine at stage 34. In the stage 34 embryo, the rectal canal that connects the spiral intestine to the rectum was closed, so the embryo will retain yolk digesta until hatch. This result was consistent with that reported in the lesser spotted dogfish, where the rectum of

embryo was closed until hatch (Mellinger et al., 1986; 1987). It is possible that embryos may achieve maximum nutrient absorption from yolk digesta by upregulating transport expression such as Slc6a19 in the posterior region of spiral intestine. In Mozambique tilapia, the neutral amino acid transporter *slc6a18* mRNA was expressed in the posterior part of intestine to complete the absorption of neutral amino acids, supporting our notion (Orozco et al., 2018).

Since yolk is directly transferred into the spiral intestine, it is assumed that anterior parts of the digestive tract, such as the esophagus and stomach, are not used during embryogenesis in the lecithotrophic cloudy catshark. Our histological observations revealed that the position equivalent to the esophagus was closed throughout the embryonic period. Consistent with our results, the digestive tract anterior to the spiral intestine appears to be inactive in the spiny dogfish embryo (Tewinkel, 1943). Immunoreactive signals for the gastric proton pump (H^+/K^+-ATPase), which represents the functional marker of stomach activity, were first detected at stage 34 in lesser spotted dogfish embryos (Gonçalves et al., 2019). In contrast, embryos of many viviparous species drink or eat nutrient materials supplied from the mother (Fujita, 1981; Hamlett et al., 2011), meaning that their esophagus and stomach must be active even during the embryonic period. Collectively, cartilaginous fish embryos during the yolk-dependent period most likely take a strategy to use only the posterior part of digestive tract, and may close a connection between spiral intestine and oral cavity. This strategy may have an advantage to reduce the cost of innate immunity inside the digestive tract, as seawater, rich in microorganisms and pathogens, would not come into the digestive tract from the oral cavity. Indeed, it has been reported that gut-associated lymphomyeloid tissue develops before the onset of feeding in the lesser spotted dogfish embryo, which is much later compared to the development of other immune systems (Lloyd-Evans, 1993).

The pre-hatching event: turning point of physiological function in embryonic body

Pre-hatching is a unique feature of cartilaginous fish among metazoans (Lechenault et al., 1993). Previously our understanding of the physiological purpose of pre-hatching or opening of the eggshell to the environment was to facilitate circulation of seawater and improve respiration (Diez and Davenport, 1987), and/or to make room for the growing embryo within the egg case (Mellinger et al., 1986; 1989). The immune system is considered to be functional before the pre-hatching event, as immunoglobulin positive cells are detected in most of lymphomyeloid system (liver, interrenal, thymus, spleen, and Leydig organ) in the lesser spotted dogfish embryo (Lloyd-Evans, 1993). In relation to respiratory function, the cloudy catshark and port Jackson shark, *Heterodontus portusjacksoni*, embryos begin buccal pumping, just after the pre-hatching event (Tomita et al., 2014; Rodda and Seymour, 2008).

In the present study, we clearly showed that pre-hatching is a turning point for embryonic nutritional absorption; after pre-hatching, embryos incorporate yolk into their intestine to digest and absorb nutrient from their yolk sac. A similar "shift" has been described for the production of urea from the extraembryonic yolk sac membrane to the embryonic liver, a crucial osmolyte for marine cartilaginous fish necessary for survival in seawater (Takagi et al., 2014; 2017). Lechenault et al. (1993) suggested that pre-hatching is comparable to hatching of anamniotes because pre-hatching occurs as a result of the degradation of a solid layer. Our findings on changes in physiological function after pre-hatching in the embryo support this notion. It is probable that pre-hatching in oviparous cartilaginous fish is a key window in embryonic development as they are for the first time exposed to the environment but remain within the eggshell for further development and growth prior to emergence.

ACKNOWLEDGEMENTS

We sincerely thank all the staff of Oarai Aquarium for their kind support for providing experimental animals, Professor S. Kuraku and staff of the Laboratory for Phyloinformatics, RIKEN BDR, for providing nucleotide sequences of cloudy catshark. We also thank Professor W.G. Anderson of University of Manitoba for critical comments on the manuscript.

FUNDING

This study was supported by a Grant-in-Aid for Scientific Research from the Japan Society for the Promotion of Science (JSPS KAKENHI 26650110, 26291065, 17H03868) to SH.

AUTHOR CONTRIBUTIONS

Conceptualization: Y.H., W.T., S.H.; Investigation: Y.H., W.T., M.K.S.W., N.O.; Resources: K.T. and K.K.; Writing - original draft: Y.H., W.T., S.H; Writing - review & editing: Y.H., W.T., M.K.S.W., S.H.; Funding acquisition: S.H. All authors contributed to the interpretation of the data and the final manuscript editing.

COMPETING INTERESTS

The authors declare no competing or financial interests.

REFERENCES

Ahn, H., Yamada, Y., Okamura, A., Tsukamoto, K., Kaneko, T. and Watanabe, S. (2013). Intestinal expression of peptide transporter 1 (PEPT1) at different life stages of Japanese eel, *Anguilla japonica*. *Comp. Biochem. Physiol. Part - B Biochem. Mol. Biol.* **166**, 157-164.

Argyriou, T., Clauss, M., Maxwell, E. E., Furrer, H. and Sánchez-Villagra, M. R. (2016). Exceptional preservation reveals gastrointestinal anatomy and evolution in early actinopterygian fishes. *Sci. Rep.* **6**, 1-10.

Babel, J. S. (1966). Reproduction, life history, and ecology of the round stingray, *Urolophus halleri* Cooper. *Fish Bull.* **137**, 1-104.

Ballard, W. W., Mellinger, J. and Lechenault, H. (1993). A series of normal stages for development of *Scyliorhinus canicula*, the lesser spotted dogfish (Chondrichthyes: Scyliorhinidae). *J. Exp. Zool.* **267**, 318-336.

Belghit, I., Skiba-Cassy, S., Geurden, I., Dias, K., Surget, A., Kaushik, S., Panserat, S. and Seiliez, I. (2014). Dietary methionine availability affects the main factors involved in muscle protein turnover in rainbow trout (*Oncorhynchus mykiss*). *Br. J. Nutr.* **112**, 493-503.

Bertin, L. (1958). Appareil digestif. In *Traité de zoologie vol 13.* (ed. P. P. Grassé), pp. 1248-1302. París: Masson et Cie Éditeurs.

Bröer, A., Klingel, K., Kowalczuk, S., Rasko, J. E., Cavanaugh, J. and Bröer, S. (2004). Molecular cloning of mouse amino acid transport system B^0, a neutral amino acid transporter related to Hartnup disorder. *J. Biol. Chem.* **279**, 24467-24476.

Bröer, S. (2008). Amino acid transport across mammalian intestinal and renal epithelia.

Physiol. Rev. **88**, 249-286.

Bucking, C. and Schulte, P. M. (2012). Environmental and nutritional regulation of expression and function of two peptide transporter (PepT1) isoforms in a euryhaline teleost. *Comp. Biochem. Physiol. -Part A Mol. Integr. Physiol.* **161**, 379-387.

Chatchavalvanich, K., Marcos, R., Poonpirom, J., Thongpan, A. and Rocha, E. (2006). Histology of the digestive tract of the freshwater stingray *Himantura signifer* Compagno and Roberts, 1982 (Elasmobranchii, Dasyatidae). *Anat. Embryol. (Berl).* **211**, 507-518.

Clements, K. D. and Raubenheimer, D. (2006). Feeding and nutrition. In *The Physiology of Fishes* (ed. D. H. Evans., J. B. Claiborne. and S. Currie), pp. 47-82. Florida: CRC Press.

Compagno, L., Dando, M. and Fowler, S. (2005). A field guide to the sharks of the world. pp34-37.

Conrath, C. L. and Musick, J. A. (2012). Reproductive biology of elasmobranchs. In *Biology of Sharks and Their Relatives, 2nd edn* (ed. J.C. Carrier, J.A. Musick and M.R. Heithaus), pp. 291-311. Florida: CRC Press.

Craig, P. M. and Moon, T. W. (2013). Methionine restriction affects the phenotypic and transcriptional response of rainbow trout (*Oncorhynchus mykiss*) to carbohydrate-enriched diets. *Br. J. Nutr.* **109**, 402-412.

Diez, J. M. and Davenport, J. (1987). Embryonic respiration in the dogfish (*Scyliorhinus canicula L.*). *J. Mar. Biol. Assoc. U. K.* **67**, 249-261.

Edgar, R. C. (2004). MUSCLE: multiple sequence alignment with high accuracy and high throughput. *Nucleic Acids Res.* **32**, 1792-1797.

Fujita, K. (1981). Oviphagous Embryos of the Pseudocarchariid Shark , *Pseudo-carcharias kamoharai*, from the Central Pacific. *Japanese J. Icthyology.* **28**, 37-44.

Gonçalves, O., Freitas, R., Ferreira, P., Araújo, M., Zhang, G. J., Mazan, S., Cohn, M. J., Castro, L. F. C. and Wilson, J. M. (2019). Molecular ontogeny of the stomach in the catshark *Scyliorhinus canicula*. *Sci. Rep.* **9**, 1-10.

Haines, A. N., Flajnik, M. F., Rumfelt, L. L. and Wourms, J. P. (2005). Immunoglobulins in the eggs of the nurse shark, *Ginglymostoma cirratum*. *Dev. Comp. Immunol.* **29**, 417-430.

Hamlett, W. C., Musick, J. A., Eulitt, A. M., Jarrell, R. L. and Kelly, M. A. (1996). Ultrastructure of uterine trophonemata, accommodation for uterolactation, and gas exchange in the southern stingray, *Dasyatis americana*. *Can. J. Zool.* **74**, 1417-1430.

Hamlett, W. C., Kormanik, G., Storrie, M., Stevens, B. and Walker, T. I. (2011). Chondrichthyan parity, lecithotrophy and matrotrophy. In *Reproductive biology and phylogeny of Chondrichthyes: sharks, batoids, and chimaeras* (ed. W. C. Hamlett), pp. 405-421. Florida: CRC Press.

Hara, Y., Yamaguchi, K., Onimaru, K., Kadota, M., Koyanagi, M., Keeley, S. D., Tatsumi, K., Tanaka, K., Motone, F., Kageyama, Y. et al. (2018). Shark genomes provide insights into elasmobranch evolution and the origin of vertebrates. *Nat. Ecol. Evol.* **2**, 1761-1771.

Hart, H. R., Evans, A. N., Gelsleichter, J. and Ahearn, G. A. (2016). Molecular identification and functional characteristics of peptide transporters in the bonnethead shark (*Sphyrna tiburo*). *J. Comp. Physiol. B Biochem. Syst. Environ. Physiol.* **186**, 855-866.

Hasegawa, K., Kato, A., Watanabe, T., Takagi, W., Romero, M. F., Bell, J. D., Toop, T., Donald, J. A. and Hyodo, S. (2016). Sulfate transporters involved in sulfate secretion in the kidney are localized in the renal proximal tubule II of the elephant fish (*Callorhinchus milii*). *Am. J. Physiol. - Regul. Integr. Comp. Physiol.* **311**, R66-R78.

Hyodo, S., Tsukada, T. and Takei, Y. (2004). Neurohypophysial hormones of dogfish, *Triakis scyllium*: Structures and salinity-dependent secretion. *Gen. Comp. Endocrinol.* **138**, 97-104.

Hyodo, S., Kakumura, K., Takagi, W., Hasegawa, K. and Yamaguchi, Y. (2014). Morphological and functional characteristics of the kidney of cartilaginous fishes: With special reference to urea reabsorption. *Am. J. Physiol. - Regul. Integr. Comp. Physiol.* **307**, R1381-R1395.

Jhaveri, P., Papastamatiou, Y. P. and German, D. P. (2015). Digestive enzyme activities in the guts of bonnethead sharks (*Sphyrna tiburo*) provide insight into their digestive strategy and evidence for microbial digestion in their hindguts. *Comp. Biochem. Physiol. -Part A Mol. Integr. Physiol.* **189**, 76-83.

Jollie, W. P. and Jollie, L. G. (1967). Electron microscopic observations on accommodations to pregnancy in the uterus of the spiny dogfish, *Squalus acanthias*. *J. Ultrasructure Res.* **20**, 161-178.

Khanna, D. R. (2004). *Biology of Fishes.* pp. 56-63. Delhi, India: Discovery Publishing House.

Kleta, R., Romeo, E., Ristic, Z., Ohura, T., Stuart, C., Arcos-Burgos, M., Dave, M. H., Wagner, C. A., Camargo, S. R., Inoue, S. et al. (2004). Mutations in *SLC6A19*, encoding B^0AT1, cause Hartnup disorder. *Nat. Genet.* **36**, 999-1002.

Kumar, S., Stecher, G. and Tamura, K. (2016). MEGA7: molecular evolutionary genetics analysis version 7.0 for bigger datasets. *Mol. Biol. Evol.* **33**, 1870-1874.

Lechenault, H., Wrisez, F. and Mellinger, J. (1993). Yolk utilization in *Scyliorhinus canicula*, an oviparous dogfish. *Environ. Biol. Fishes* **38**, 241-252.

Leigh, S. C., Papastamatiou, Y. and German, D. P. (2017). The nutritional physiology of sharks. *Rev. Fish Biol. Fish.* **27**, 561-585.

Liu, Z., Zhou, Y., Feng, J., Lu, S., Zhao, Q. and Zhang, J. (2013). Characterization of oligopeptide transporter (PepT1) in grass carp (*Ctenopharyngodon idella*). *Comp. Biochem. Physiol. B: Biochem. Mol. Biol.* **164**, 194-200.

Lloyd-Evans, P. (1993). Development of the lymphomyeloid system in the dogfish, *Scyliorhinus canicula*. *Dev. Comp. Immunol.* **17**, 501-514.

Mellinger, J., Wrisez, F. and Alluchon-Gerard, M. J. (1986). Developmental biology of an oviparous shark, *Scyliorhinus canicula*. In *Indo- Pacific Fish Biology: Proceedings of the Second International Conference on Indo-Pacific Fishes* (ed. T. Uyeno, R. Arai, T. Taniuchi and K. Matsuura, K), pp. 310-332. Tokyo: Ichthyological Society of Japan

Mellinger, J., Wrisez, F. and Desselle, J. C. (1987). Transitory closures of esophagus and rectum during elasmobranch development: models for human congenital anomalies? *Archives de Biologie*. **98**, 209-230.

Mellinger, J., Wrisez, F., Leray, C. and Haye, B. (1989). A comparison of egg and newborn lipids in the oviparous dogfishes, *Scyliorhinus canicula* and *S. stellaris* (Chondrichthyes). Preliminary data. *Biol. Struct. Morpho.* **2**, 44.

Musick, J. A. and Ellis, J. K. (2005). Reproductive evolution of chondrichthyans. Reproductive biology and phylogeny of Chondrichthyes: sharks, batoids, and

chimaeras, 3, (ed. W. C. Hamlett), pp. 45-80. CRC Press.

Ng, A. N. Y., De Jong-Curtain, T. A., Mawdsley, D. J., White, S. J., Shin, J., Appel, B., Dong, P. D. S., Stainier, D. Y. R. and Heath, J. K. (2005). Formation of the digestive system in zebrafish: III. Intestinal epithelium morphogenesis. *Dev. Biol.* **286**, 114-135.

Okano, T., Otake, K., Teshima, K. and Mizue, S. (1981). Epithelial cells of the intestine in *Mustelus manazo* and *M. griseus* embryos. Studies on Sharks - XX. *Bull. off Fac. Fish.*, **51**, 23-28.

Orozco, Z. G. A., Soma, S., Kaneko, T. and Watanabe, S. (2017). Effects of fasting and refeeding on gene expression of *slc15a1a*, a gene encoding an oligopeptide transporter (PepT1), in the intestine of Mozambique tilapia. *Comp. Biochem. Physiol. Part - B Biochem. Mol. Biol.* **203**, 76-83.

Orozco, Z. G. A., Soma, S., Kaneko, T., and Watanabe, S. (2018). Spatial mRNA expression and response to fasting and refeeding of neutral amino acid transporters *slc6a18* and *slc6a19a* in the intestinal epithelium of Mozambique tilapia. *Front. Physiol.* **9**, 212.

Parker, T. J. (1880). On the Intestinal Spiral Valve in the genus Raia. *Trans. Zool. Soc. London* **11**, 49-61.

Perrault, C. (1671). Mémoires pour servir à l'histoire naturelle des animaux. Académie des sciences. pp. 54-58.

Rimoldi, S., Bossi, E., Harpaz, S., Cattaneo, A. G., Bernardini, G., Saroglia, M. and Terova, G. (2015). Intestinal B0AT1 (SLC6A19) and PEPT1 (SLC15A1) mRNA levels in European sea bass (*Dicentrarchus labrax*) reared in fresh water and fed fish and plant protein sources. *J. Nutr. Sci.* **4**, 1-13.

Rodda, K. R. and Seymour, R. S. (2008). Functional morphology of embryonic development in the Port Jackson shark *Heterodontus portusjacksoni* (Meyer). *J. Fish Biol.* **72**, 961-984.

Rønnestad, I., Gavaia, P. J., Viegas, C. S. B., Verri, T., Romano, A., Nilsen, T. O., Jordal, A. E. O., Kamisaka, Y. and Cancela, M. L. (2007). Oligopeptide transporter PepT1 in Atlantic cod (*Gadus morhua L.*): Cloning, tissue expression and comparative aspects. *J. Exp. Biol.* **210**, 3883-3896.

Schindelin, J., Arganda-Carreras, I., Frise, E., Kaynig, V., Longair, M., Pietzsch, T., Preibisch, S., Rueden, C., Saalfeld, S., Schmid, B. et al. (2012), Fiji: an open-source platform for biological-image analysis. *Nat. Methods.* **9**, 676-682.

Smith, H. W. (1936). the Retention and Physiological Role of Urea in the Elasmobranchii. *Biol. Rev.* **11**, 49-82.

Sveier, H., Kvamme, B. O. and Raae, A. J. (2001). Growth and protein utilization in Atlantic salmon (*Salmo salar* L.) given a protease inhibitor in the diet. *Aquacult. Nutr.* **7**, 255-264.

Takabe, S., Teranishi, K., Takaki, S., Kusakabe, M., Hirose, S., Kaneko, T. and Hyodo, S. (2012). Morphological and functional characterization of a novel Na^+/K^+-ATPase-immunoreactive, follicle-like structure on the gill septum of Japanese banded houndshark, *Triakis scyllium*. *Cell Tissue Res.* **348**, 141-153.

Takagi, W., Kajimura, M., Tanaka, H., Hasegawa, K., Bell, J. D., Toop, T., Donald, J. A. and Hyodo, S. (2014). Urea-based osmoregulation in the developing embryo of oviparous cartilaginous fish (*Callorhinchus milii*): contribution of the extraembryonic yolk sac during the early developmental period. *J. Exp. Biol.* **217**, 1353-1362.

Takagi, W., Kajimura, M., Tanaka, H., Hasegawa, K., Ogawa, S. and Hyodo, S. (2017). Distributional shift of urea production site from the extraembryonic yolk sac membrane to the embryonic liver during the development of cloudy catshark (*Scyliorhinus torazame*). *Comp. Biochem. Physiol. -Part A Mol. Integr. Physiol.* **211**, 7-16.

Terova, G., Corà, S., Verri, T., Rimoldi, S., Bernardini, G. and Saroglia, M. (2009). Impact of feed availability on PepT1 mRNA expression levels in sea bass (*Dicentrarchus labrax*). *Aquaculture* **294**, 288-299.

Teshima, K. and Tomonaga, S. (2016). Freshwater stingray embryos store yolk in their intestinal epithelial cells. *J. Natl. Fish. Univ.* **64**, 182-187.

Tewinkel, L. E. (1943). Observations on later phases of embryonic nutrition in *Squalus acanthias*. *J. Morphol.* **73**, 177-205.

Theodosiou, N. A. and Oppong, E. (2019). 3D morphological analysis of spiral intestine morphogenesis in the little skate, *Leucoraja erinacea*. *Dev. Dyn.* **248**, 688-701.

Tomita, T., Nakamura, M., Sato, K., Takaoka, H., Toda, M., Kawauchi, J. and Nakaya, K. (2014). Onset of buccal pumping in catshark embryos: How breathing develops in the egg capsule. *PLoS One* **9**, 1-9.

Verri, T., Kottra, G., Romano, A., Tiso, N., Peric, M., Maffia, M., Boll, M., Argenton, F., Daniel, H. and Storelli, C. (2003). Molecular and functional characterisation of the zebrafish (*Danio rerio*) PEPT1-type peptide transporter. *FEBS Lett.* **549**, 115-122.

Wallace, K. N., Akhter, S., Smith, E. M., Lorent, K. and Pack, M. (2005). Intestinal growth and differentiation in zebrafish. *Mech. Dev.* **122**, 157-173.

Walton, K. D., Freddo, A. M., Wang, S. and Gumucio, D. L. (2016). Generation of intestinal surface: an absorbing tale. *Development* **143**, 2261-2272.

Wetherbee, B. M., Gruber, S. H. and Ramsey, A. L. (1987). X- radiographic observations of food passage through digestive tracts of lemon sharks. *Trans. Am. Fish. Soc.* **116**, 763-767.

White, E. G. (1937). Interrelationships of the elasmobranchs with a key to the order Galea. *Bull Am Mus Nat Hist* **74**, 25-138.

Wilson, J. M. and Castro, L. F. C. (2010). Morphological diversity of the gastrointestinal tract in fishes. In Fish physiology (Vol. 30, pp. 1-55). Academic Press.

Xu, X., Qin, Y., Luo, G., Huang, X., Zou, W. Z., Zheng, L., Wang, J. and Su, Y. (2015). Ontogeny of digestive organs during early developmental stages of the tropical whitespotted bamboo shark, *Chiloscyllium plagiosum* - a histological study. *Mar. Freshw. Behav. Physiol.* **48**, 253-266.

Xu, D., He, G., Mai, K., Zhou, H., Xu, W. and Song, F. (2016). Expression pattern of peptide and amino acid genes in digestive tract of transporter juvenile turbot (*Scophthalmus maximus L.*). *J. Ocean Univ. China* **15**, 334-340.

Figures

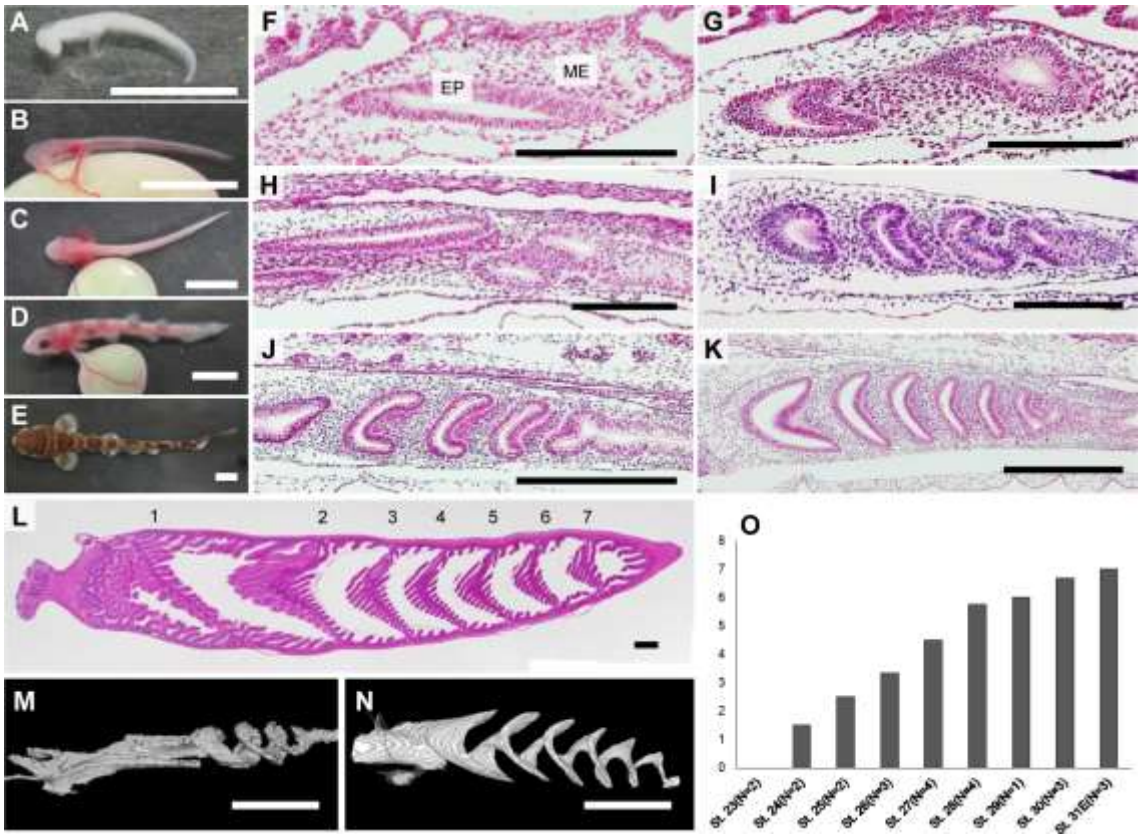

Figure 1. Developing spiral intestine of cloudy catshark embryo. Representative developing embryos at stage 25 (A), stage 28 (B), stage 31L (C), stage 32 (D)and hatched fish (E) are shown. (F)-(L) Sections of developing spiral intestine stained with hematoxylin and eosin. Left side represents rostral region. (F) Stage 23. Pseudostratified epithelium (EP) composing a straight intestinal tract and mesenchyme (ME) were distinguishable. (G) Two-separated luminal spaces indicating a spiral turn were observed in stage 24 embryo. (H) to (J) represent spiral intestines of stages 25, 27 and 29, respectively. The numbers of turns increased along with the progress of development. (K) The number of spiral turns reached to 7 at stage 31E, which is

identical to that of juvenile intestine (L). 3D reconstruction image of intestinal lumen of stage 27 (M) and stage 31E (N). (O) Developmental changes in the number of spiral turns. Scale bars=1 cm (A, B, C, D, E), 250 μm (F, G, H, I) and 500 μm (J, K, L, M, N).

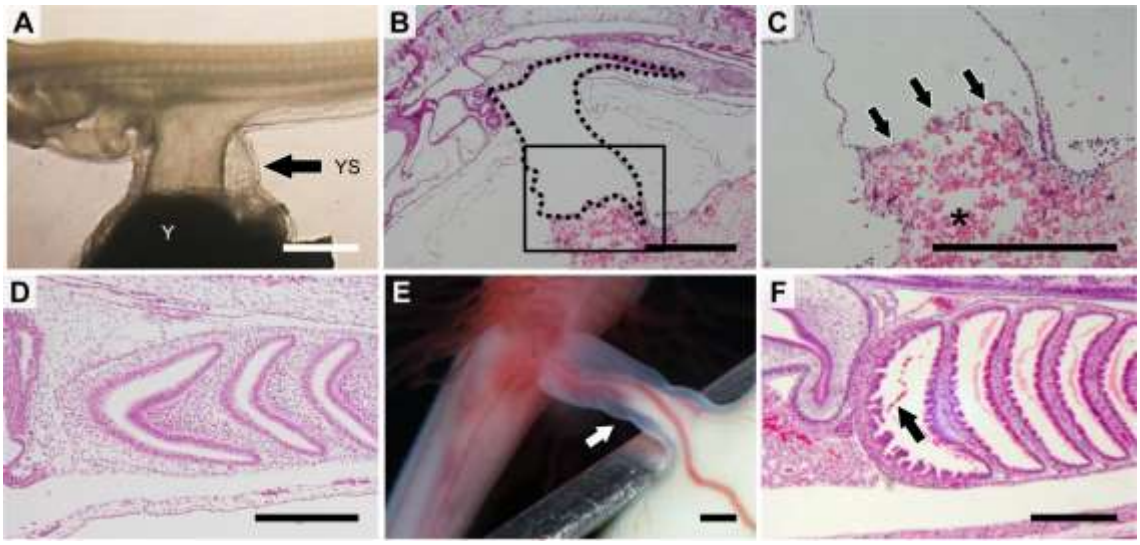

Figure 2. Yolk inflow into the intestine. (A) Stage 23 embryo (Left side represents rostral region). External yolk sac is connected with embryo by yolk stalk (YS). (B) Hematoxylin and eosin staining section of stage 24 embryo. Broken line indicates intestinal lumen directly connected with yolk stalk. (C) Enlarged view of the boxed area in (B). Arrows indicate membranous lid preventing yolk (asterisk) inflow into the embryonic intestine. (D) Sagittal section of stage 31E embryo intestine showing no eosinophilic yolk inside the intestine. (E) Light yellow-colored yolk was observed inside the yolk stalk in stage 31L embryo just after pre-hatching (arrow). (F) Section of the stage 31L embryo intestine. Eosinophilic yolk granules are visible in the intestinal lumen (arrow).

Y: Yolk, YS: Yolk stalk. Bar = 1 mm (A, B and D) and 500 μm (C, E and F).

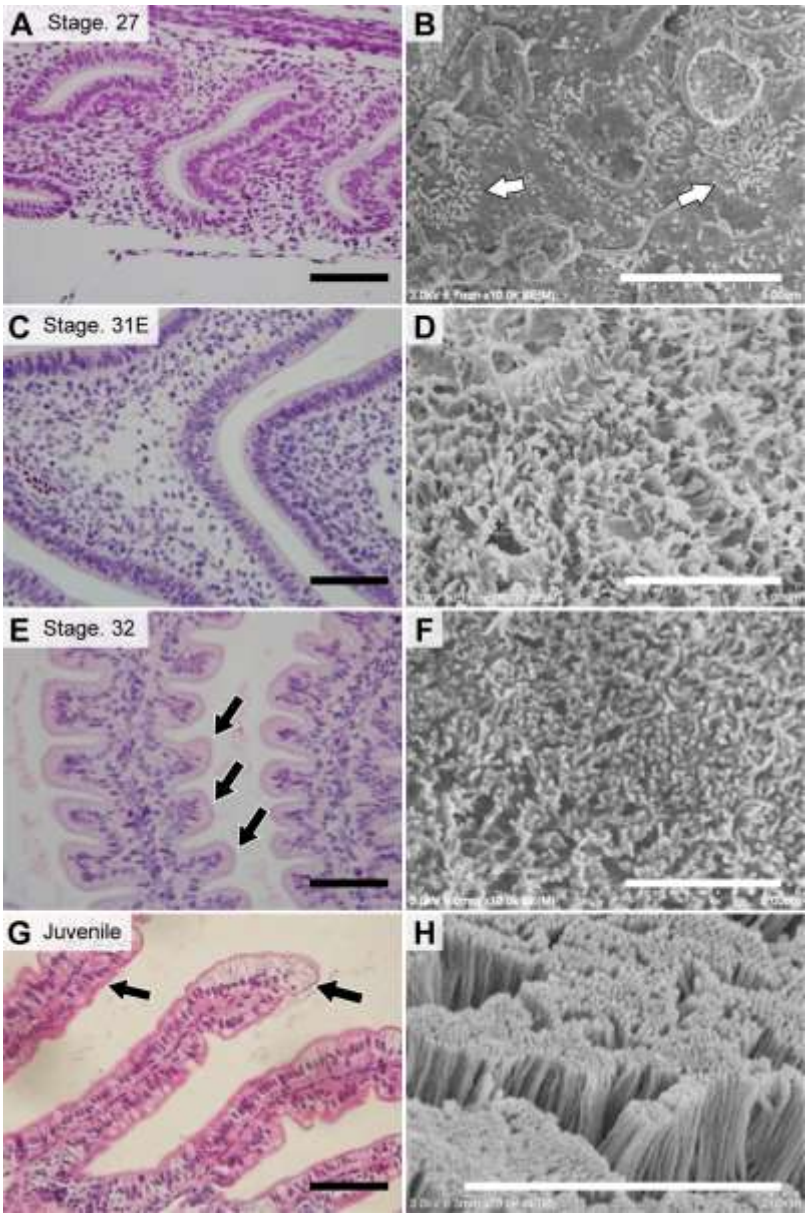

Figure 3. Formation of secondary fold and microvilli. (A), (C), (E), (G) Sections of intestine of embryos and juvenile. Black arrows indicate secondary fold. (B), (D), (F), (H) Scanning electron micrographs of intestinal epithelium of embryos and juvenile. White arrows indicate emerging microvilli. Bar = 100 μm (A, C, E, G) and 5 μm (B, D, F, H).

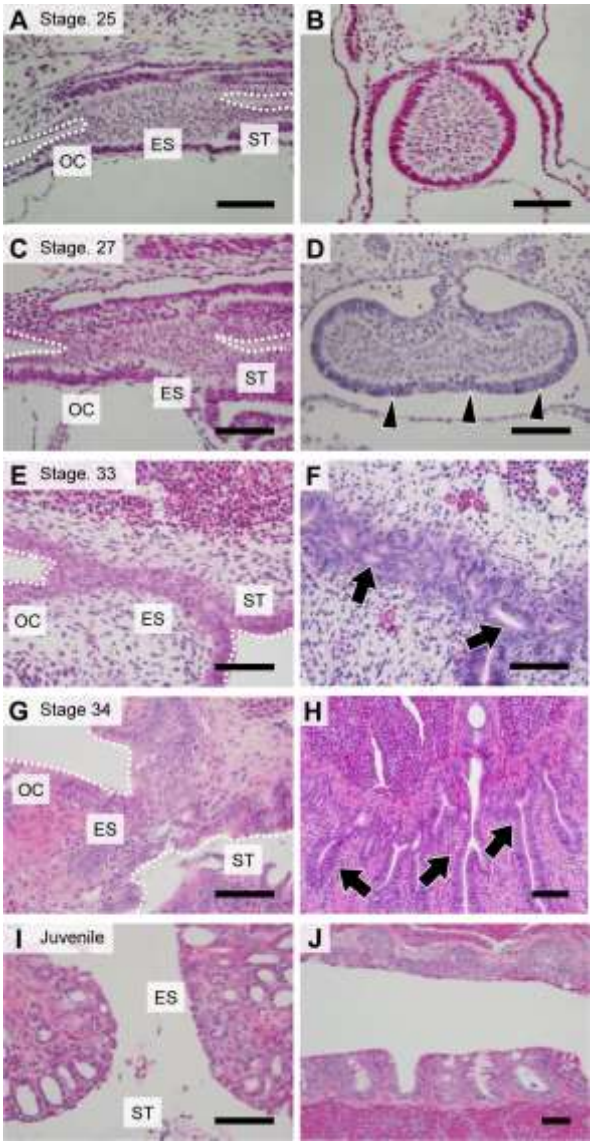

Figure 4. Esophagus opening. Sagittal (A, C, E, G, I) and cross sections (B, D, F, H, J) of esophagus (ES) of embryos and juvenile. Left side represents rostral region in sagittal sections. Luminal surface of oral cavity (OC) and Stomach (ST) are indicated with white dotted lines. Arrowheads represent epithelium, while arrows represent gaps between dorsal and ventral sides of esophagus. Bar = 100 µm.

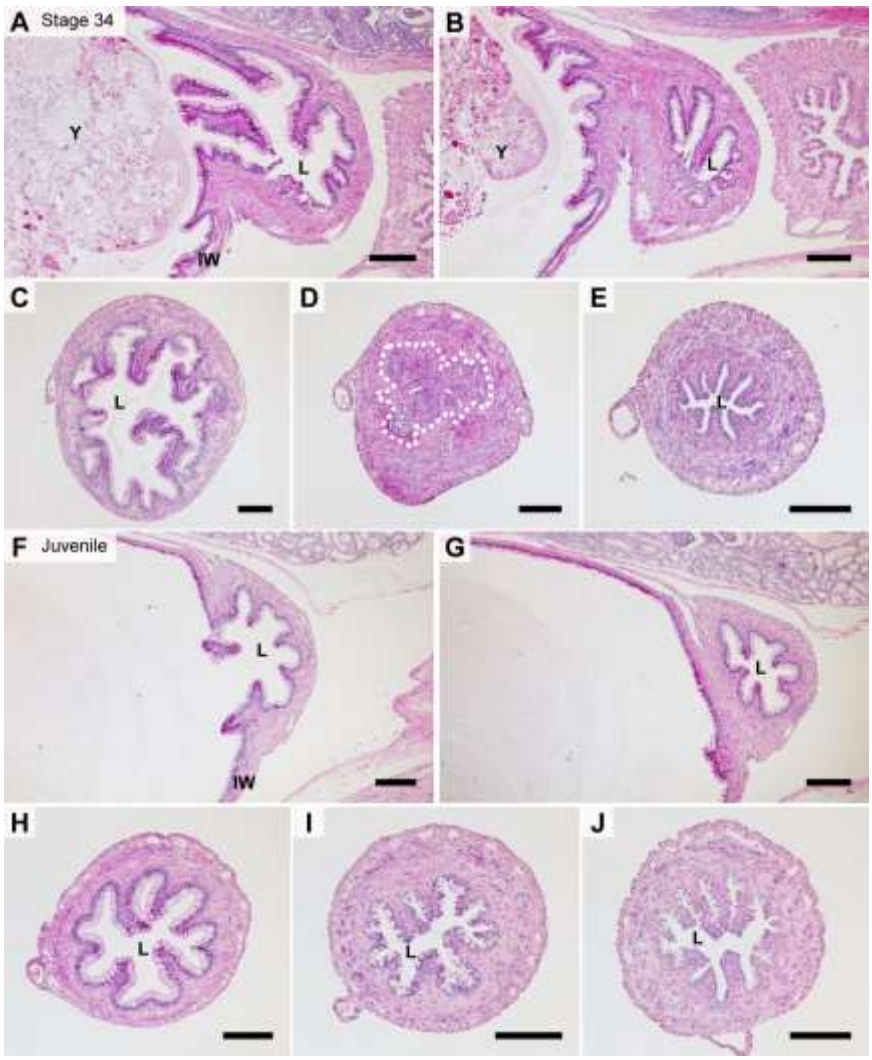

Figure 5. Connection between spiral intestine and rectum. Sagittal sections of posterior part of the spiral intestine (A, B, F, G) and transverse sections of the posteriormost portion of spiral intestine (C, H), the rectal canal (D, I) and the anteriormost portion of rectum (E, J). (A-E) represent stage 34 embryo and (F-J) are juvenile. The closed mucosal area in the rectal canal is indicated with white dotted line. IW: intestinal wall, L: lumen, Y: yolk. Bar = 200 μm.

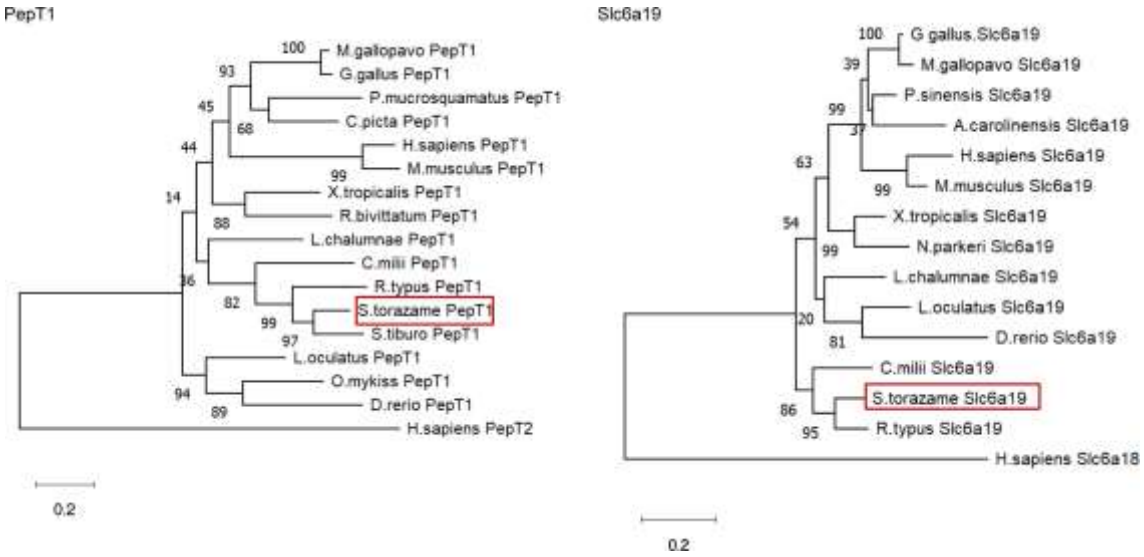

Figure 6. Molecular phylogenetic tree of vertebrate PepT1 and Slc6a19. Bootstrap probabilities are shown next to the branches. The accession numbers of genes used in the analysis are listed in Table S2. The cloudy catshark sequences are shown with red box. Homo sapiens PepT2 and Slc6a18 were used as the outgroup.

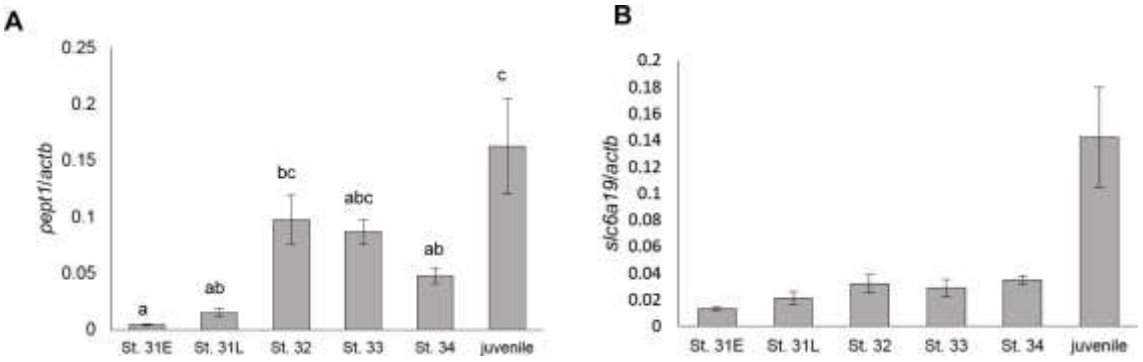

Figure 7. Changes in expression of *pept1* (A) and *slc6a19* (B) mRNAs in the developing spiral intestine. The mRNA levels were shown as the relative values to the mRNA levels of β-actin. Data are presented as means±s.e.m of *n*=5. Different characters on graphs indicate that there is a significant difference. ($p < 0.05$)

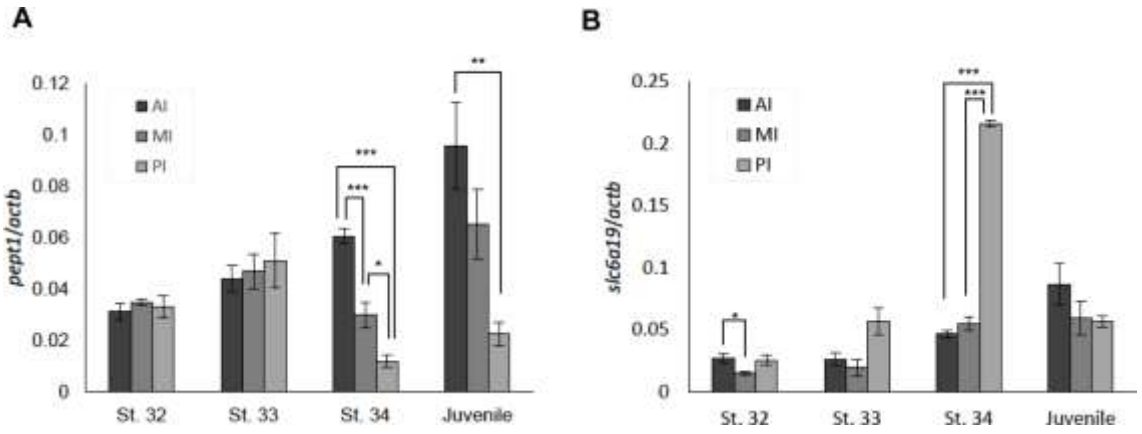

Figure 8. The mRNA levels of *pept1* and *slc6a19* in the developing spiral intestine. (A) and (B) Developmental changes in the relative mRNA levels of *pept1* (A) and *slc6a19* (B) to those of *β-actin*. Intestines were separated into the three segments, and mRNA levels in each segment were analyzed. AI: Anterior intestine, MI: Middle intestine, PI: Posterior intestine. Data are presented as means±s.e.m of n=5. Statistically significant differences are shown with asterisks. *P < 0.05, **P < 0.01, ***P < 0.001.

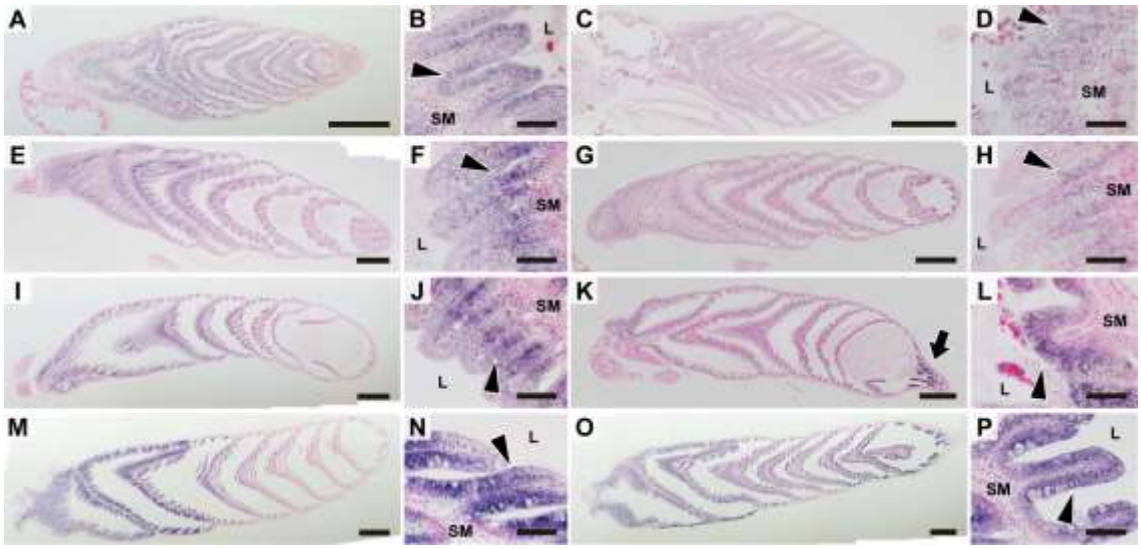

Figure 9. *In situ* hybridization analyses of *pept1* and *slc6a19* mRNA in the developing spiral intestine. The *pept1* (A, B, E, F, I, J, M, N) and *slc6a19* (C, D, G, H, K, L, O, P) mRNA signals in stage 32 (A-D), stage 33 (E-H), stage 34 (I-L), and juvenile (M-P). (B, D, F, H, J, L, N, P) represent magnified views of (A, C, E, G, I, K, M, O), respectively. Left side represents rostral region in sagittal sections. Sections were counterstained with Nuclear Fast Red. Arrow indicates signals in the posterior most of intense. Arrowheads indicate signals in the epithelial cells. L: lumen, SM: submucosa. Bar = 1 mm (A, C, E, G, I, K, M, O) and 100 μm (B, D, F, H, J, L, N, P).

Table S1. Primer sets used in the present study

Target			Amplicon (bp)
Primer sets for molecular cloning (5′ to 3′)			
st*pepT1*	Sense:	ATTCAGCCTGATCAGATGCAGA	895
	Antisense:	CCTGGAGCACTGATTTCATGTTG	
st*slc6a19*	Sense:	TGGGCTGTGCTGTATGTATG	678
	Antisense:	AGAAAGTCCGAGGCAGAATAAC	
st*actb*	Sense:	TGGTTGGTATGGGACAGAAAG	934
	Antisense:	ATCTGCTGGAAGGTGGAAAG	
Primer sets for real-time qPCR assay (5′ to 3′)			
st*pepT1*	Sense:	ACCCTTCCTATCTTCCCTACC	121
	Antisense:	CCTCAGATGGTGCCAGTAAAT	
st*slc6a19*	Sense:	TGGGCTGTGCTGTATGTATG	88
	Antisense:	TCTACCCTCCCTTATCTTGTCC	
st*actb*	Sense:	CCTGGCATTGCAGACCGTAT	73
	Antisense:	GCAATGATCTTGATTTTCATGGTACT	

Target gene abbreviations: PepT1, peptide transporter 1; Slc6a19, solute carrier family 6a19; actb, β-actin.

Table S2. The accession numbers of genes used in the analysis

Gene name	Accession Number
Scyliorhinus torazame Slc15a1	LC507941
Sphyrna tiburo Slc15a1	KX216515.1
Rhincodon typus Slc15a1	XM_020512255.1
Callorhinchus milii Slc15a1	XM_007906296.1
Homo sapiens solute carrier family 15 (oligopeptide transporter), member 1	BC096329.3
Mus musculus Pept1	AF205540.1
Meleagris gallopavo PepT1	AY157977.1
Gallus gallus PEPT1	KF366603.1
Oncorhynchus mykiss SLC15A1	KY775396.1
Danio rerio Slc15a1	AY300011.1
Xenopus tropicalis Slc15a1	XM_012957717.1
Rhinatrema bivittatum SLC15A1	XM_029604484.1
Protobothrops mucrosquamatus SLC15A1	XM_015810135.1
Chrysemys picta bellii SLC15A1	XM_005303909.3
Lepisosteus oculatus Slc15a1	XM_015363348.1
Latimeria chalumnae SLC15A1	XM_005992304.1
Scyliorhinus torazame Slc6a19	LC507942
Rhincodon typus B(0)AT1	XP_020367154
Callorhinchus milii B(0)AT1	XP_007887825
Homo sapiens SLC6A19	NM_001003841.3
Mus musculus Slc6a19	NM_028878.4
Gallus gallus SLC6A19	XM_419056.6
Meleagris gallopavo SLC6A19	XM_010708607.2
Lepisosteus oculatus Slc6a19	XM_006635651.2
Latimeria chalumnae SLC6A19	XM_014498080.1
Danio rerio Slc6a19a.1	NM_001098178.1
Xenopus tropicalis Slc6a19	NM_001127113.1
Pelodiscus sinensis SLC6A19	XM_006137063.3
Anolis carolinensis Slc6a19	XM_003219814.3
Nanorana parkeri SLC6A19	XM_018568852.1
Homo sapiens PepT2	NM_021082
Homo sapiens Slc6a18	NM_182632

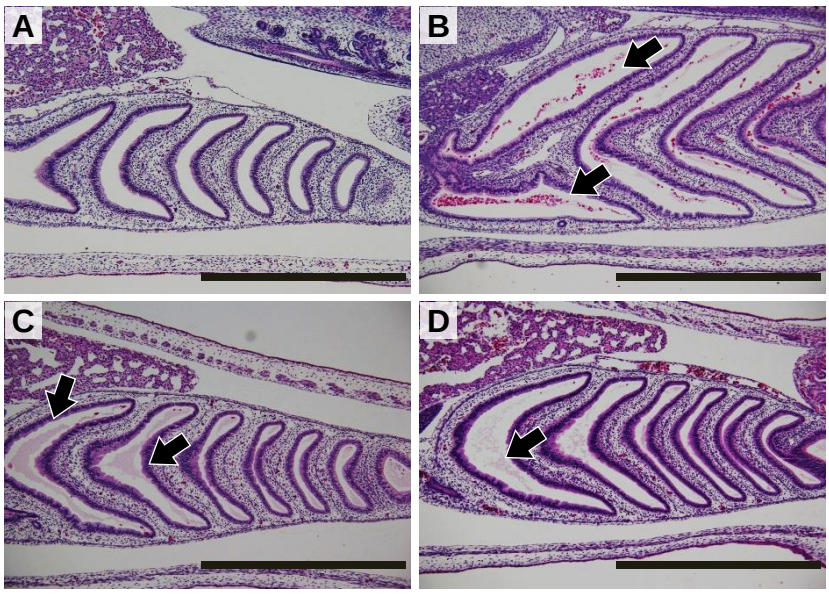

Figure S1. Yolk inflow occurred nearly pre-hatching period. Sections of the intestine. (A) and (B) Sections of the intestine of stage 31L embryos within 24 hours after pre-hatching. (C) and (D) Sections of the intestine of stage 31L embryos within 48 hours after pre-hatching. Arrows indicate yolk inside the intestinal lumen. Bar = 1mm.

Table S1. Primer sets used in the present study

Target			Amplicon (bp)
Primer sets for molecular cloning (5′ to 3′)			
st*pepT1*	Sense:	ATTCAGCCTGATCAGATGCAGA	895
	Antisense:	CCTGGAGCACTGATTTCATGTTG	
st*slc6a19*	Sense:	TGGGCTGTGCTGTATGTATG	678
	Antisense:	AGAAAGTCCGAGGCAGAATAAC	
st*actb*	Sense:	TGGTTGGTATGGGACAGAAAG	934
	Antisense:	ATCTGCTGGAAGGTGGAAAG	
Primer sets for real-time qPCR assay (5′ to 3′)			
st*pepT1*	Sense:	ACCCTTCCTATCTTCCCTACC	121
	Antisense:	CCTCAGATGGTGCCAGTAAAT	
st*slc6a19*	Sense:	TGGGCTGTGCTGTATGTATG	88
	Antisense:	TCTACCCTCCCTTATCTTGTCC	
st*actb*	Sense:	CCTGGCATTGCAGACCGTAT	73
	Antisense:	GCAATGATCTTGATTTTCATGGTACT	

Target gene abbreviations: PepT1, peptide transporter 1; Slc6a19, solute carrier family 6a19; actb, β-actin.

Table S2. The accession numbers of genes used in the analysis

Gene name	Accession Number
Scyliorhinus torazame Slc15a1	LC507941
Sphyrna tiburo Slc15a1	KX216515.1
Rhincodon typus Slc15a1	XM_020512255.1
Callorhinchus milii Slc15a1	XM_007906296.1
Homo sapiens solute carrier family 15 (oligopeptide transporter), member 1	BC096329.3
Mus musculus Pept1	AF205540.1
Meleagris gallopavo PepT1	AY157977.1
Gallus gallus PEPT1	KF366603.1
Oncorhynchus mykiss SLC15A1	KY775396.1
Danio rerio Slc15a1	AY300011.1
Xenopus tropicalis Slc15a1	XM_012957717.1
Rhinatrema bivittatum SLC15A1	XM_029604484.1
Protobothrops mucrosquamatus SLC15A1	XM_015810135.1
Chrysemys picta bellii SLC15A1	XM_005303909.3
Lepisosteus oculatus Slc15a1	XM_015363348.1
Latimeria chalumnae SLC15A1	XM_005992304.1
Scyliorhinus torazame Slc6a19	LC507942
Rhincodon typus B(0)AT1	XP_020367154
Callorhinchus milii B(0)AT1	XP_007887825
Homo sapiens SLC6A19	NM_001003841.3
Mus musculus Slc6a19	NM_028878.4
Gallus gallus SLC6A19	XM_419056.6
Meleagris gallopavo SLC6A19	XM_010708607.2
Lepisosteus oculatus Slc6a19	XM_006635651.2
Latimeria chalumnae SLC6A19	XM_014498080.1
Danio rerio Slc6a19a.1	NM_001098178.1
Xenopus tropicalis Slc6a19	NM_001127113.1
Pelodiscus sinensis SLC6A19	XM_006137063.3
Anolis carolinensis Slc6a19	XM_003219814.3
Nanorana parkeri SLC6A19	XM_018568852.1
Homo sapiens PepT2	NM_021082
Homo sapiens Slc6a18	NM_182632

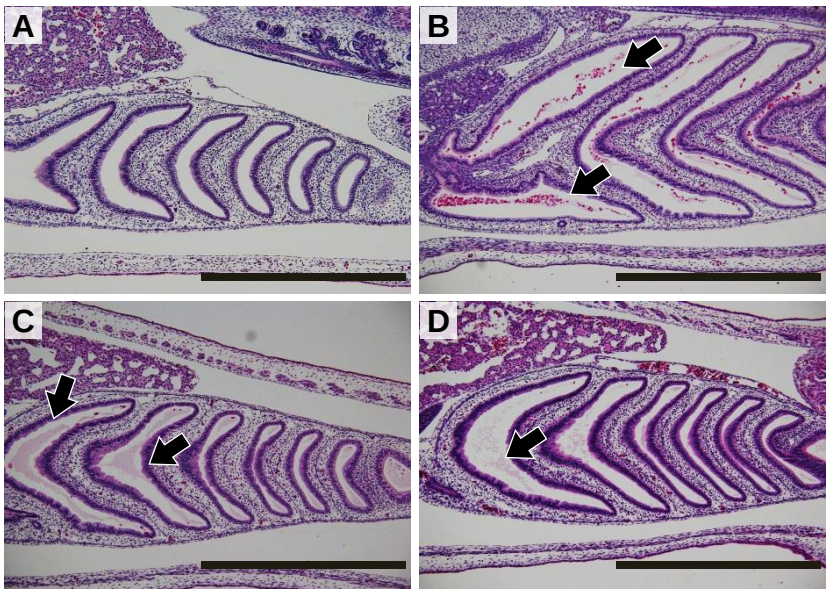

Figure S1. Yolk inflow occurred nearly pre-hatching period. Sections of the intestine. (A) and (B) Sections of the intestine of stage 31L embryos within 24 hours after pre-hatching. (C) and (D) Sections of the intestine of stage 31L embryos within 48 hours after pre-hatching. Arrows indicate yolk inside the intestinal lumen. Bar = 1mm.